

Artificially Structured Materials III: Patterned Structures

Laura Heyderman, Chairman

A study of magnetic interactions of $\text{Ni}_{80}\text{Fe}_{20}$ arrays using ultrasensitive microcantilever torque magnetometry

L. Gao, D. Q. Feng, L. Yuan, T. Yokota, R. Sabirianov, and S. H. Liou^{a)}
*Department of Physics and Astronomy and Center for Materials Research and Analysis,
University of Nebraska, Lincoln, Nebraska 68588*

M. D. Chabot, D. Porpora, and J. Moreland
National Institute of Standards and Technology, Boulder, Colorado 80305

(Presented on 8 January 2004)

We have successfully fabricated single and paired $300\text{ nm}\times 1.5\text{ }\mu\text{m}\times 32\text{ nm}$ $\text{Ni}_{80}\text{Fe}_{20}$ bars on a microcantilever using focused ion beam milling. Magnetic interactions of the paired bars were studied by using magnetic force microscopy, microcantilever torque magnetometry, and micromagnetic simulation. Our results clearly indicate that the magnetic switching behavior of the paired $\text{Ni}_{80}\text{Fe}_{20}$ bars is affected by magnetostatic interactions. The magnetic hysteresis curves for a sample with eight pairs of $\text{Ni}_{80}\text{Fe}_{20}$ bars consist of a series of stable switching states that are related to the domain wall motion in the bars. © 2004 American Institute of Physics.
[DOI: 10.1063/1.1682912]

I. INTRODUCTION

Measuring micrometer and submicrometer scale magnetic features has proven to be a challenge for conventional magnetometers. Thus, more sensitive methods are needed to probe magnetism on this scale.¹⁻⁵ Microcantilever torque magnetometry (MTM) based on a torsion-mode atomic force microscope (AFM) is a promising experimental technique for measuring submicrometer magnetism due to its higher sensitivity than SQUID magnetometry.³⁻⁵

The main challenge of this measurement technique is obtaining well-defined micromagnetic samples on cantilevers. Chabot *et al.* have created a process in which film deposition is combined with the cantilever fabrication process.⁶ This method requires using multistep photolithography process.

The interaction of submicrometer-sized arrays is an important topic for micromagnetism. Much work has been done in this area.⁷⁻⁹ However, due to measurement sensitivity limitations, arrays of hundreds of elements must be fabricated to obtain a high enough signal-to-noise ratio. The results are often clouded by statistical variations such as dot shape, size, and spacing. Due to its high sensitivity, MTM is expected to reduce the statistical variations of the magnetic interaction by studying just a few pairs of magnetic particles.

In this work, we use focused ion beam (FIB) milling, a simple one-step method, to prepare submicrometer bars on the microcantilever and use magnetic force microscopy

(MFM), microcantilever torque magnetometry, and micromagnetic simulation to study the magnetic reversal behavior of these bars.

II. EXPERIMENT

We start with a microcantilever which already has a $7\text{ }\mu\text{m}\times 7\text{ }\mu\text{m}\times 32\text{ nm}$ $\text{Ni}_{80}\text{Fe}_{20}$ film deposited on the top left corner [Fig. 1(a)]. The $\text{Ni}_{80}\text{Fe}_{20}$ film was then patterned by a FIB workstation using a Ga^+ liquid metal ion source operated at 30 keV ion energy. The ion beam current was approximately 70 pA. A patterning software package allowed us to generate the milled pattern from a bitmap image. The $\text{Ni}_{80}\text{Fe}_{20}$ films were patterned into 12 single $300\text{ nm}\times 1.5\text{ }\mu\text{m}\times 32\text{ nm}$ bars [Fig. 1(b)] and 8 pairs of $300\text{ nm}\times 1.5\text{ }\mu\text{m}\times 32\text{ nm}$ bars [Figs. 1(c)]. The milling time was 5 min for both patterns. The gaps between the edges of bars are $1\text{ }\mu\text{m}$ for single bars and 40 nm for paired bars.

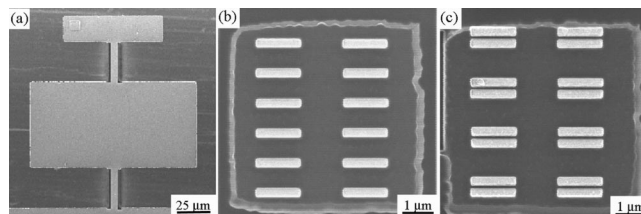


FIG. 1. (a) Microcantilever with $\text{Ni}_{80}\text{Fe}_{20}$ film deposited on the top left corner. (b) Focused ion beam patterned $\text{Ni}_{80}\text{Fe}_{20}$ arrays with 12 single $300\text{ nm}\times 1.5\text{ }\mu\text{m}\times 32\text{ nm}$ bars and (c) eight pairs of $300\text{ nm}\times 1.5\text{ }\mu\text{m}\times 32\text{ nm}$ bars with gap of 40 nm between adjacent bars.

^{a)}Author to whom correspondence should be addressed. electronic mail: sliou@unl.edu

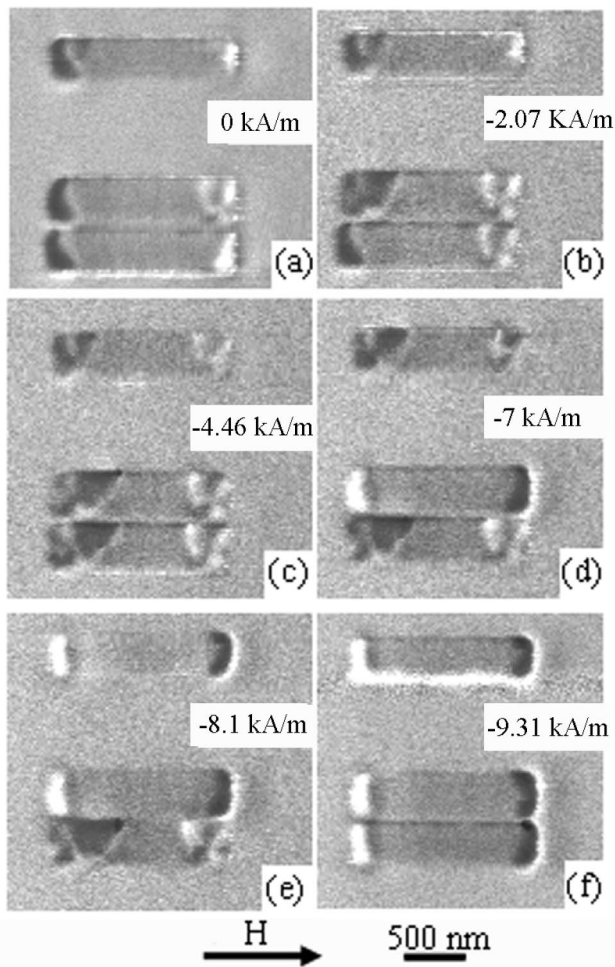


FIG. 2. Field dependent magnetic domain structures of single $\text{Ni}_{80}\text{Fe}_{20}$ bars ($300 \text{ nm} \times 1.5 \mu\text{m} \times 32 \text{ nm}$) and same size paired bars with a gap of 40 nm. The sample was saturated with a field of 79.6 kA/m along the long axis of the bars and then decreased to (a) 0 kA/m, (b) -2.07 kA/m , (c) -4.46 kA/m , (d) -7 kA/m , (e) -8.1 kA/m , and (f) -9.31 kA/m .

Field dependent magnetic domain images were obtained under ambient conditions with a commercial magnetic force microscopy. Magnetic properties of the patterned $\text{Ni}_{80}\text{Fe}_{20}$ films were characterized using a microcantilever torque magnetometer in vacuum. All measurements were done with a magnetic field applied along the long axis of the bars. Micromagnetic simulations were performed to study the magnetization reversal of the paired $\text{Fe}_{20}\text{Ni}_{80}$ bars using the OOMMF software package developed by NIST.¹⁰

III. RESULTS AND DISCUSSION

Figure 2 shows the domain structures of a single and a set of paired $300 \text{ nm} \times 1.5 \mu\text{m} \times 32 \text{ nm}$ $\text{Ni}_{80}\text{Fe}_{20}$ bars under different magnetic fields. All the MFM images were obtained using tapping/lift mode with CoPt MFM tips at a lift height of 20 nm. The tip's north pole points down, perpendicular to the sample surface. According to the MFM contrast mechanism,¹¹ the magnetization direction of the bars is from dark to light. The $300 \text{ nm} \times 1.5 \mu\text{m} \times 32 \text{ nm}$ single bars and paired bars with a 40 nm gap are observed simultaneously. The sample was saturated with a field of 79.6 kA/m along the long axis of the bars. At zero field, the magnetization

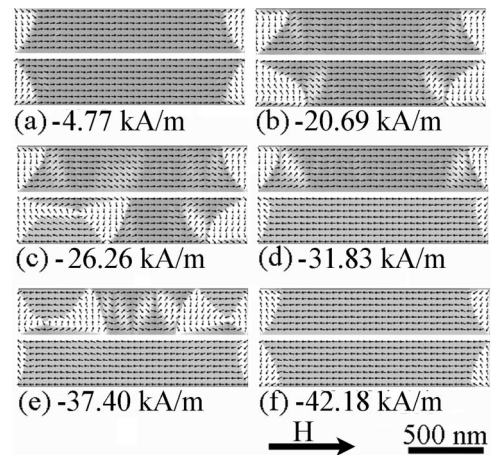


FIG. 3. Micromagnetic simulations was performed on the paired $\text{Ni}_{80}\text{Fe}_{20}$ bars ($300 \text{ nm} \times 1.5 \mu\text{m} \times 32 \text{ nm}$) with a gap of 40 nm. The sample was saturated along the long axis of the bars and then decreases to (a) -4.77 kA/m , (b) -20.69 kA/m , (c) -26.26 kA/m , (d) -31.83 kA/m , (e) -37.40 kA/m , and (f) -42.18 kA/m .

direction of the bars did not change and was still along the direction of the applied magnetic field [Fig. 2(a)]. As the field switched to negative, end domains and vortices were formed first [Fig. 2(b)], then domain walls propagate along the bars [Fig. 2(c)] and are stopped by the pinning sites. The pinning sites could be produced by surface or edge roughness, defects, or disorder in the film (such as random anisotropy). The magnetic reversal process for the bars is domain wall motion instead of coherent rotation. At a field of -7 kA/m , only one of the paired bars is reversed [Fig. 2(d)]. As field changed to -8.1 kA/m , the single bar reversed [Fig. 2(e)], but the magnetization direction of paired bars is still antiparallel to each other. At larger negative field, all the bars switched [Fig. 2(f)]. The fact that the switching field of single bars is larger than the reversing field of only one of the paired bars and less than that of both paired bars shows that the magnetostatic interaction exists between the closely paired bars. The interaction makes the antiparallel magnetization directions of paired bars a stable state.

To clarify the magnetization reversal of the paired bars, we performed micromagnetic simulations with the following parameters. The magnetization of $\text{Fe}_{20}\text{Ni}_{80}$ was 800 kA/m, the anisotropy constant was $4.5 \times 10^3 \text{ J/m}^3$, and the exchange constant was $1.3 \times 10^{-13} \text{ J/m}^3$.¹² We used a random anisotropy setup to mimic the real medium. The results also show that the switching of each bar in the paired bars system is not independent. After saturation, paired bars form a symmetrically inverted C state at the remanent state [C state is named because the domain structure resembles the letter C, Fig. 3(a)]. With the negative field applied, the magnetization reversal proceeds through the formation of two vortices (end domains) [Figs. 3(b) and 3(c)]. Due to the broken symmetry (random anisotropy), the reversal of one of the bars happens first [Fig. 3(d)]. Although the general picture of the reversal of this bar is similar to the single bar case, there are some deviations because of the interactions with the second bar. Due to the magnetostatic interactions, the system creates a closure for the magnetic field (magnetization of paired bars

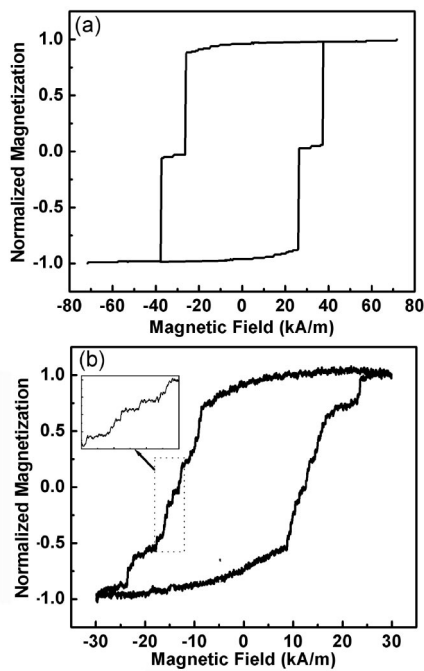


FIG. 4. (a) Simulated magnetic hysteresis loop of the paired $\text{Ni}_{80}\text{Fe}_{20}$ bars ($300\text{ nm}\times 1.5\text{ }\mu\text{m}\times 32\text{ nm}$) with a gap of 40 nm. (b) Hysteresis loop of the eight sets of paired bars with same size is obtained with a microcantilever torque magnetometer. Inset: Close-up view of series of stable switching states.

is aligned in opposite directions). It is a stable state for the system of paired bars. Then at somewhat larger applied field, the system is forced out of this potential well and the second bar also switches [Fig. 3(f)]. The simulation results are consistent with the MFM measurement.

Figure 4(a) shows a simulated hysteresis loop for one set of paired bars system. The two steps during the reversal is caused by the magnetostatic interaction between the paired bars, which is correlated with the domain structures shown in Figs. 2 and 3. Figure 4(b) shows the M - H curve obtained with microcantilever torque magnetometry for a cantilever with eight sets of paired bars patterned on the 32 nm film, as shown in Fig. 1(c). The hysteresis curves are obtained by sweeping the external field from -31.83 kA/m to $+31.83\text{ kA/m}$. The torque field and cantilever resonant frequency used are 85 A/m and 25.4 kHz , respectively. We have yielded a saturation magnetization of 870 kA/m for the eight sets of paired bars with a magnetic volume of $2.3\times 10^{-19}\text{ m}^3$. The experimental magnetization is within 10% of the bulk value of 800 kA/m . The error may be due to difficulty in estimating the thickness of the film and the actual value of the torque

field. The observed series of stable switching states during the magnetization reversal process is likely due to the domain wall motion in the bars. A possible explanation for the difference between the simulation and the measured loop is that the simulation is performed only on one paired bars under ideal conditions but MTM includes all the switching of eight paired bars in which each bar may have a different reversal field due to different defect structures formed during the FIB processing.

IV. CONCLUSIONS

The focused ion beam milling is a convenient way to obtain arbitrary patterns on a microcantilever. Domain structure and micromagnetic simulation results show that the reversal of the paired $300\text{ nm}\times 1.5\text{ }\mu\text{m}\times 32\text{ nm}$ bars is affected by the magnetostatic interactions. We used MTM to measure eight sets of paired $\text{Ni}_{80}\text{Fe}_{20}$ bars. The hysteresis curve consists of a series of stable switching states. This is related to the domain wall motion in the bars. We show that microcantilever torque magnetometry is a suitable method for measuring magnetic interactions in submicrometer-sized magnetic samples. Future work will improve the sensitivity of the MTM by optimizing the cantilevers. This will allow the study of the magnetization reversal of only one set of paired bars.

ACKNOWLEDGMENTS

Research was supported by NSF MRSEC Award Nos. DMR-0213808 and DMR-0116780 and Army Research Office DAAD Grant No. 19-03-1-0298. T. Yokota was supported by a Grant-in-Aid for JSPS Fellows, Grant No. 00000652.

- ¹B. C. Stipe, H. J. Mamin, T. D. Stowe, T. W. Kenny, and D. Rugar, *Phys. Rev. Lett.* **86**, 2874 (2001).
- ²J. G. E. Harris, D. D. Awschalom, F. Matsukura, H. Ohno, K. D. Maranowski, and A. C. Gossard, *Appl. Phys. Lett.* **75**, 1140 (1999).
- ³M. Löhndorf, J. Moreland, P. Kabos, and N. Rizzo, *J. Appl. Phys.* **87**, 5995 (2000).
- ⁴M. D. Chabot and J. Moreland, *J. Appl. Phys.* **93**, 7897 (2003).
- ⁵J. Moreland, *J. Phys. D* **36**, R39 (2003).
- ⁶M. D. Chabot and J. T. Markert, *Proc. SPIE* **3875**, 104 (1999).
- ⁷J. F. Smyth, S. Schultz, D. R. Fredkin, D. P. Kern, S. A. Rishton, H. Schmid, M. Cali, and T. R. Koehler, *J. Appl. Phys.* **69**, 5262 (1991).
- ⁸S. Y. Chou and L. Kong, *J. Appl. Phys.* **79**, 5855 (1996).
- ⁹V. Novosad, M. Grimsditch, J. Darrouzet, J. Pearson, S. D. Bader, V. Metlushko, K. Guslienko, Y. Otani, H. Shim, and K. Fukamichi, *Appl. Phys. Lett.* **82**, 3716 (2003).
- ¹⁰J. Donahue and R. D. McMichael, *Physica B* **233**, 272 (1997).
- ¹¹S. H. Liou and Y. D. Yao, *J. Magn. Magn. Mater.* **190**, 130 (1998).
- ¹²M. Klaui, C. A. F. Vaz, L. Lopez-Diaz, and J. A. C. Bland, *J. Phys.: Condens. Matter* **15**, 985 (2003).